Image Analysis based on Radon-type Integral Transforms Over Conic Sections

Dhekra El Hamdi[1,2], Mai K. Nguyen[1], Hedi Tabia[1] and Atef Hamouda[2]
[1]*Laboratoire Equipes de Traitement de l'Information et Système (ETIS), Université de Cergy-Pontoise/ ENSEA/ CNRS UMR 8051, F-95000 Cergy-Pontoise, France*
[2]*Laboratoire d'Informatique, Programmation, Algorithmique et Heuristiques (LIPAH), Faculté des Sciences de Tunis, Université de Tunis EL Manar, 1068, Tunis, Tunisia*

Keywords: Radon Transform, Conic Sections, Image Analysis, Feature Extraction.

Abstract: This paper presents a generalized Radon transform defined on conic sections called Conic Radon Transform (CRT) for image analysis. The proposed CRT extends the classical Radon transform (RT) which integrates a image function $f(x,y)$ over straight lines. As the CRT is capable of detecting conic sections with any position and orientation in original images it makes possible to build a new descriptor based on integrating an image over conic sections. In order to test and verify the utility and performance of this new approach we have developed, in this work, the Radon transforms defined on circles and on parabolas, then built a descriptor combining the features extracted by the circular RT, parabolic RT and linear RT. This descriptor is applied to object classification. A number of experiments on both synthetic and real datasets illustrates the efficiency and the advantages of this new approach taking into account the global features of different (circular, parabolic and linear) shapes of images under study.

1 INTRODUCTION

One of the most basic stages in image analysis is the detection of primitives features such as lines and curves in an image. The most popular method for segment recognition is the classical Radon transform (RT) (Radon, 1917) which is defined as an integral of the image function along all lines in image space.
In fact, various applications based on the RT were implemented such as centerline detection (Zhang and Couloigner, 2007), biometric identification such as iris identification (Bharath et al., 2014) and object recognition (Nguyen and Hoang, 2015).
So far the classical RT is restricted to segment detection. In this paper, we focus on curves detection. Our main motivation is to achieve both of the two following objectives: definition of a generalized Radon transform which detects more complex curves than lines, and application of this new transform to feature extraction. Our purpose consists to verify that integrating an object over curves rather than lines can improve the performance of object classification.
This paper is organized as follows: Section 2 presents a review of related works in the literature. Afterwards, Section 3 defines the RT over conic sections. In section 4, we discuss the use of our approach for feature extraction. Then, we present the experimental evaluation of our method in section 5. Section 6 concludes the paper.

2 RELATED WORKS

In this section, we review some previous works related to RT for feature extraction and generalized Radon transform.
In the evolution of image analysis, a number of methods have been proposed for definition of descriptors which have high discrimination power.
There are two main categories of feature extraction methods: a transform-based methods which computes a global descriptor of the shape, and a handcrafted -based methods which aim at extracting local features such as Scale Invariant Features Transform (SIFT), Gradient Localization Oriented Histogram (GLOH) and Gradient Moments (GM) (Islam and Sluzek, 2010) . These descriptors are local and based on gradient magnitude and orientation of keypoints.
In this paper, we focus on the first category which aims to extract the global descriptor. In contrast to

Hamdi, D., Nguyen, M., Tabia, H. and Hamouda, A.
Image Analysis based on Radon-type Integral Transforms Over Conic Sections.
DOI: 10.5220/0006613403560362
In *Proceedings of the 13th International Joint Conference on Computer Vision, Imaging and Computer Graphics Theory and Applications (VISIGRAPP 2018) - Volume 4: VISAPP*, pages 356-362
ISBN: 978-989-758-290-5

local features, global features are not based on certain points of interest but they describe the image as a whole.

Popular methods are based on Fourier transform, the Generic Fourier Descriptor (GFD) proposed by Zhang and Lu is a typical Fourier descriptor which is invariant to shape rotation (Zhang and Lu, 2002).

Besides the Fourier descriptor, the classical RT has also been employed for the definition of several shape descriptors due to its excellent geometric properties.

Hasegawa et al. proposed a RT- based method for shape recognition which is based on the histogram of RT (Hasegawa and Tabbone, 2016). This approach is robust to translation, rotation and scaling but it not invariant under shape distortion. For that, the authors compute an angle correlation matrix and apply the dynamic time warping to the angle coordinate in order to be robust to distortion transformations. Furthermore, the RT is used for near-duplicate image detection (Lei et al., 2014). The authors proposed a family of geometric invariant features based on linear RT. These features are able to distinguish images which are not near- duplicated pairs.

Despite the efficiency of RT for linear features detection, it remains limited in detection of more complex features. The recognition of different patterns than linear features can not be achieved directly by RT.

One of the most used transforms for the detection of complex features is the generalized Hough Transform (GHT) (Ballard, 1981). It can recognize parameterized curves and arbitrary shapes from binary images and from grey level images. However, the GHT is a discrete intuitive method unlike the RT which is based on a mathematic foundation allowing to recover a continuous 2D function f through its integrals.

Recently, several works have focused on generalizing the RT to detect more complex patterns where the straight lines were replaced by curves and weight functions were introduced into the integrals along these curves.

Elouedi et al. defined a discrete generalized Radon transform for detection of polynomial curves (PDRT) (Elouedi et al., 2015). This transform generalizes the classical RT by projecting the image with respect to polynomial curves. However, the use of the PDRT is limited to square prime sized images.

Our motivation in this work is to define a novel generalized Radon transform. Our transform can detect complex forms which are the conic sections. We present an analytical method for generalized Radon transform which is very different to the approach mentioned above.

In the next section, we introduce the definition of a generalized Radon transform which is the extension of the classical RT to conic sections in the plane. We provide the mathematical framework to the integrals over conic sections.

3 RADON TRANFORM OVER CONIC SECTIONS

Let us first recall the classical Radon transform (RT). The RT in euclidean space represents the integration of a function $f(x,y)$ over lines as defined in this equation:

$$Rf(\rho,\phi) = \int_{-\infty}^{+\infty}\int_{-\infty}^{+\infty} f(x,y)\delta(\rho - xcos(\phi) - ysin(\phi))dxdy, \quad (1)$$

where $\delta(.)$ is the Dirac delta function, $\rho \in]-\infty,+\infty[$ is the distance from the origin of the coordinate system to the line and $\phi \in [0,\pi[$ is an angle corresponding to the orientation of the line (Fig. 1).

In Radon space the value $Rf(\rho,\phi)$ reaches a maximum value (peak) at the points who coordinates ρ and ϕ correspond to the lines parameters (ρ,ϕ) (Fig. 2).

Let : T_{x_0,y_0}, R_{ϕ_0}, S_α the geometric transformations where $\overrightarrow{u}(x_0,y_0)$: the translation vector of coordinates (x_0,y_0), ϕ_0 : the rotation angle, α : the scale factor, and $g(x',y')$: the transformed function $f(x,y)$.

The RT offers excellent properties that are useful for object recognition as outlined below:

- Symmetry : $Rf(\rho,\phi) = Rf(-\rho,\phi \pm \pi)$.
- Periodicity : $Rf(\rho,\phi) = Rf(\rho,\phi + 2k\pi)$, of period 2π, k is integer.
- Translation : a translation of $f(x,y)$ by $\overrightarrow{u}(x_0,y_0)$: $g = T_{x_0,y_0}[f]$ implies a shift by a distance $d = x_0\cos\phi + y_0\sin\phi$ in ρ coordinate $\Rightarrow Rg(\rho,\phi) = Rf(\rho - x_0\cos\phi - y_0\sin\phi,\phi)$.
- Rotation : a rotation by an angle ϕ_0 of $f(x,y)$: $g = R_{\phi_0}[f]$ implies a shift in ϕ coordinate $\Rightarrow Rg(\rho,\phi) = Rf(\rho,\phi+\phi_0)$.
- Scaling : a zoom of factor $\alpha \neq 0$ in $f(x,y)$: $g = S_\alpha[f]$ involves a change of scale in ρ coordinate and in Rg amplitude by a factor α and $\frac{1}{|\alpha|}$ respectively $\Rightarrow Rg(\rho,\phi) = \frac{1}{|\alpha|}Rf(\alpha\times\rho,\phi)$.

As arbitrary curves can not be detected by the RT, a generalized Radon transform over conic sections (CRT) in two dimensions may be able to detect more complex curves than lines. Whereas the classical RT of a function integrates over lines, the generalized Radon transform represents the integration over conic sections.

The proposed CRT transform extends the formalism

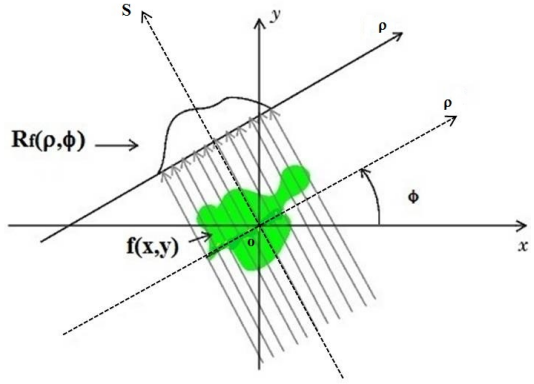

Figure 1: Geometry of the Radon transform over lines.

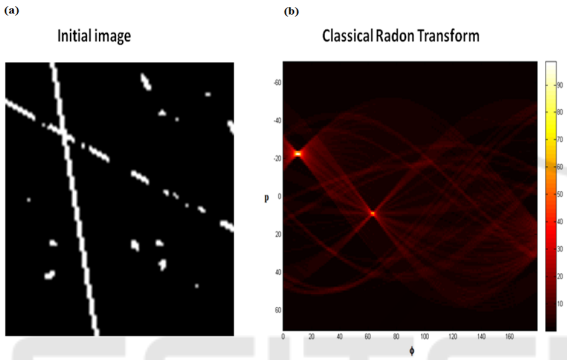

Figure 2: (a) Initial image presenting two lines. (b) The classical RT of the image represented in (a): the coordinates of each peak corresponds to polar parameters of line in (a).

of the RT presented in (Cormack, 1981). Cormack defined a generalized Radon transform which is defined on general set of curves in the plane. This last include special cases of parabolas, hyperbolas, straight lines and circles through the origin with some restrictions. In fact, theses parabolas and hyperbolas curves are given in polar coordinates with one focus is fixed at the origin of the polar coordinate system.

3.1 The CRT Formalism

Geometrically a conic section is the locus of all points M whose distance to the focus F is equal to a constant e (eccentricity) multiplied by the distance from M to the directrix of the conic (Fig. 3).

The conic section in polar coordinates with focus at the origin, is defined as:
for $M(r,\theta)$:

$$r = \frac{\rho}{1 + e\ cos(\theta - \phi)}, \qquad (2)$$

where

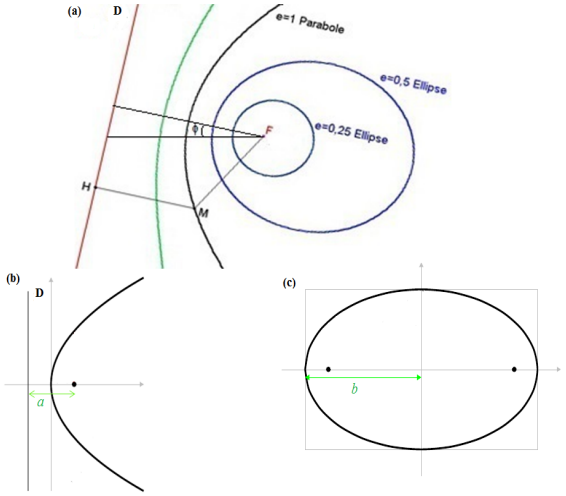

Figure 3: (a) Four conic with same focus and their directrix: ellipses ($e = 0.25$, $e = 0.5$), parabola ($e = 1$) and hyperbola ($e = 2$) with fixed focus F and directrix D. (b) Parabola according to angle $\phi 1 = 180°$. (c) Ellipse according to angle $\phi 2 = 0°$.

$$\rho = \begin{cases} b(1-e^2) \\ a \\ b(e^2-1) \end{cases} for \begin{cases} 0 \le e < 1,\ \theta \in]-\pi, \pi[\\ e = 1,\ \theta \in]-\pi, \pi[\\ e > 1,\ \theta \in]-\theta_0, \theta_0[\cup \\ \quad]\theta_0, 2\pi - \theta_0[,\ cos(\theta_0) = \frac{1}{e} \end{cases}$$

a is the distance from the focus to the directrix for parabola and b is the semi major axis for ellipse and hyperbola.
The generalized Radon transform integrates a function $f(x,y)$ over conic sections in the plane. It is defined as:

$$R_c f(x_F, y_F, \rho, \phi, e) = \int_c f(x,y) ds, \qquad (3)$$

where ds denotes the integration measure on this conic section.

$$x = \frac{\rho}{1 + e\ cos(\theta - \phi)} cos(\theta).$$

$$y = \frac{\rho}{1 + e\ cos(\theta - \phi)} sin(\theta).$$

Let :

$$\gamma = \theta - \phi,\ ds = \sqrt{dr^2 + r^2 d\gamma^2},$$

$$dr^2 + r^2 d\gamma^2 = r^2 d\gamma^2 \frac{1 + e^2 + 2\ e\ cos(\gamma)}{(1 + e\ cos(\gamma))^2}.$$

$$\Rightarrow\ ds = \rho \frac{\sqrt{1 + e^2 + 2\ e\ cos(\gamma)}}{(1 + e\ cos(\gamma))^2} d\gamma.$$

We find:

$$R_c f(x_F, y_F, \rho, \phi, e) = \int_\gamma f \left(\frac{\rho}{1 + e\ cos(\gamma)} cos(\gamma + \phi) + x_F, \frac{\rho}{1 + e\ cos(\gamma)} sin(\gamma + \phi) + y_F \right) \rho \frac{\sqrt{1 + e^2 + 2\ e\ cos(\gamma)}}{(1 + e\ cos(\gamma))^2} d\gamma. \quad (4)$$

Therefore the CRT space is expressed by five parameters which are the coordinates of focus x_F and y_F, the conic parameter ρ, the orientation angle of conic ϕ and the eccentricity e.

3.2 Numerical Simulation Results

We describe in this section the numerical implementation of the RT over conic sections. For that throughout the paper, we present only the discretisation of a class of conic with fixed focus (x_F, y_F) and fixed eccentricity e.

For the special case of $e = 1$, $x_F = y_F = 0$, we integrate over parabolas with focus at the origin. The equation of CRT become:

$$R_c f(\rho, \phi) = \int_\gamma f \left(\frac{\rho}{1 + cos(\gamma)} cos(\gamma + \phi), \frac{\rho}{1 + cos(\gamma)} sin(\gamma + \phi) \right) \frac{\rho \sqrt{2 + 2\ cos(\gamma)}}{(1 + cos(\gamma))^2} d\gamma. \quad (5)$$

The original image function $f(x,y)$ of size $Nx \times Ny$ is discretized as follows: $Nx = Ny = 100$ (arbitrary length unit), $dx = dy = 1$, $-50 \leq x \leq 49$ and $-50 \leq y \leq 49$. The central point in the CRT coincides with the origin of coordinates of the object $(x,y) = (0,0)$.

The CRT requires integrals that must be computed numerically (Equation (5)). This last is performed via the summations a long γ using a discretisation angular step $d\gamma = 1rad$. When points in the summation grid do not fit those of the discrete function, a linear interpolation method is used to calculate the values of the function at the new positions.

Therefore, to treat the general CRT transform we have applied this previous discretisation iteratively by varying eccentricity e and the focus coordinates x_F and y_F.

The proposed transform is illustrated with some numerical results based on synthetic images (Fig. 4, Fig. 5).

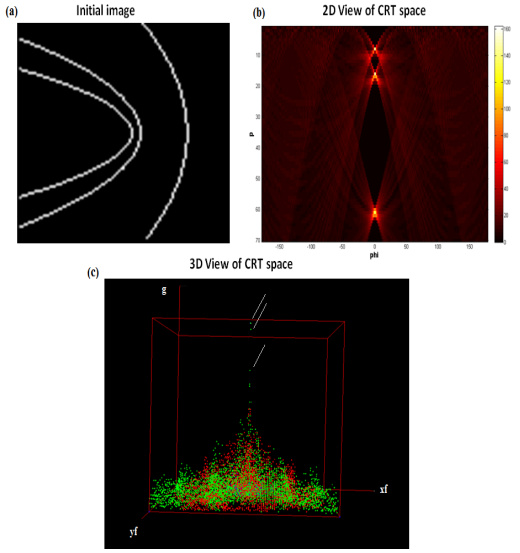

Figure 4: (a) Initial image where three parabolas are positioned at the center row. The result of the CRT on (a) is the $(x_F, y_F, \rho, \phi, e)$ parameters space where (b) present 2D view of CRT space ($e = 1$, $x_F = y_F = 0$) and the coordinates of each of the peaks corresponds to the parameters (ϕ, ρ) of the curves. ρ is the distance of focus to directrix and ϕ is the orientation of parabola. (c) present 3D view of CRT space according to $(x_F, y_F, R_c f((x_F, y_F, \rho, \phi, e))$ where the color corresponds to the eccentricity e (blue: ellipse, green: parabola, red: hyperbola) and the peaks which have green color corresponds to parabolas.

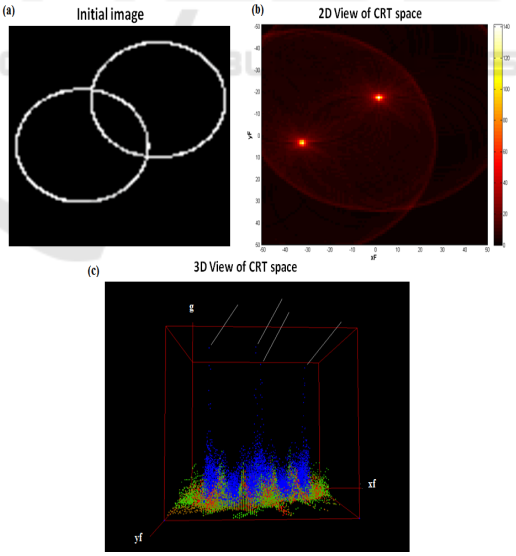

Figure 5: (a) Initial image where two ellipses are presented. (b) 2D view shows the peaks corresponding to the position of one focus for each ellipse. (c) The coordinates of each of the maximum value correspond to the parameters $(x_F, y_F, R_c f((x_F, y_F, \rho, \phi, e))$ of the four focus of ellipses according to $(\phi = 0°, e = 0.5, \rho = 22)$. The peaks have blue color which corresponds to ellipses.

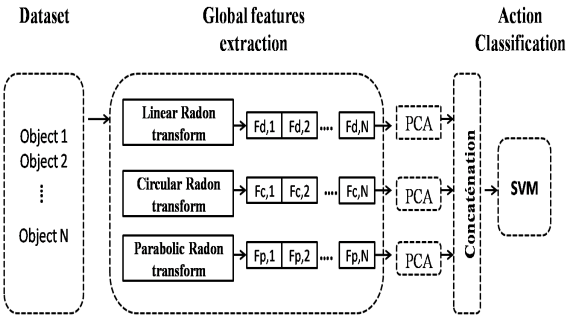

Figure 6: Architecture of proposed approach.

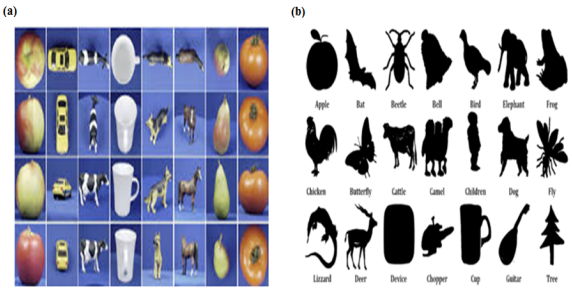

Figure 7: (a) Classes of ETH-80 data set. (b) Classes of MPEG-7 data set.

4 APPLICATION TO FEATURE EXTRACTION

The proposed approach for feature extraction relies on a set of global features extracted from Radon space. The main contribution of this work is to present the utility of integrating an image over curves other than lines. In this section, we proposed a novel descriptor based on CRT transform.

Our approach can be divided into two stages, as outlined in Fig. 6. In the first stage, we extracted global features and in the second stage, the resulting features are concatenated and then given to the Support Vector Machine(SVM) classifier.

The global features are extracted directly from Radon space. In order to deal with generic shapes, we chose the integration over circles and parabolas rather than lines.

For each focus, the result of parabolic Radon transform is a (ϕ, ρ) Radon space. we varied the angle ϕ in $[0, 179°[$ and ρ in $[1, \sqrt{N_x^2 + N_y^2}]$. N_x, N_y are the size of image. Futhermore, the result of circular Radon transform which is a special case of ellipse is a vector of radius R. We varied the radius R in $[-\sqrt{N_x^2 + N_y^2}, \sqrt{N_x^2 + N_y^2}]$.

In order to reduce the computational time of CRT transform, first we applied CRT over parabolas and circles with one fixed focus which is the centroid of image. Then we varied the number of focus in order to increase the performance of our descriptor.

We transformed the parabolic Radon space in a vector (Fp) and also the circular Radon space in a vector (Fc).

Therefore, for each object, a set of global features are extracted which are parabolic features (Fp), circular features (Fc) and also linear features (Fd) which is a vector given by the classical Radon space.

We applied principal component analysis (PCA) to the Fp, Fc and Fd vectors for all objects existing in dataset in order to reduce the dimensionality of vectors. We combined all features into a one final features vector. The goal of the features concatenation stage is to extract discriminant information that improves the object classification accuracy compared to features extracted from only linear RT.

In the classification step, we used a standard SVM (Chang and Lin, 2011) using the radial basis function kernel.

5 EXPERIMENTS

To evaluate the effectiveness of our approach for object classification, we carried out the experiments on two image data sets: ETH-80, and MPEG-7 data set. Some examples of objects in these datasets are shown in Fig 7. The main motivation behind the selection of these two databases is that they present a good benchmark to show how the proposed descriptor can handle multi-object categorization tasks.

On the first, ETH- 80 dataset contains eight different object categories: apples, tomatoes, pears, toy-cows, toy-horses, toy-dogs, toy-cars and cups. Each category is represented by 10 objects and 41 views per object are provided. For the qualitative analysis of our descriptor, we input to our system the same repartition of datasets as those used in methods we compared with and display our results with their ones. In fact, four randomly chosen images from each of 10 objects (in total 40 images) are selected for the classification set. The remaining instances constitute the training set.

In training phase, we have putted the parameters C and γ of SVM classifier respectively to 8 and 0.0625.

To evaluate the proposed approach, we used the $F-measure$ which is a robust measure to evaluate the performance of a descriptor for object class recognition. It is defined by:

$$F - measure = \frac{2\,tp}{po + tp + fp}, \qquad (6)$$

Table 1: $F-measure$ for ETH80 classes.

Object	SIFT	GLOH	GM	RT	CRT
Apple	0.97	0.93	0.91	0.80	0.96
Car	0.99	0.97	0.96	0.98	1
Cow	0.98	0.95	0.82	0.87	0.93
Cup	0.99	0.97	0.97	1	1
Dog	0.97	0.92	0.87	0.88	0.93
Horse	0.98	0.94	0.87	0.82	0.91
Pear	0.98	0.95	0.95	0.98	1
Tomato	0.98	0.96	0.88	0.78	0.95
Average	0.98	0.95	0.90	0.89	0.96

Table 2: Overall accuracy on ETH80 dataset with training 50% and test 50%.

Training	Test	Overall Acuracy		
		SIFT (Setitra and Larabi, 2015)	RT	CRT
50%	50%	90%	86%	90%

where tp is the number of true positive, fp is the number of false positive and po is the number of positive examples of each class to the classifier.
In this repartition of dataset, we presented 40 images as positive examples and 40×7 images as negative examples for each class. The average measure of our descriptor outperforms the descriptor based only on classical RT.
The average $F-measure$ of our approach is 0.96 versus 0.89 for the RT based method (Table 1).
We compared then the $F-measure$ of our descriptor with some state of the art techniques, namely : SIFT, GLOH and GM which were experimented on the same dataset. Table 1 gives the $F-measure$ for each class in the first ETH- 80 dataset. Table 1 shows that SIFT has a better average score than our descriptor relatively to the ETH- 80 dataset. However, we mention the difference is slight and in some classes, $F-measure$ with the CRT-descriptor outperforms the one of SIFT descriptor. This slight difference is mainly due to the miscategorization of dogs, horses, and cows owing to the similarity of animal legs.
Besides, we have done several experiments with respect to different sizes of labelled set and test set. From Table 2, it can be observed that the overall accuracy of our descriptor is similar to the rate of SIFT descriptor for equal division (50% training, 50% test).

Moreover, we evaluated our approach on MPEG-7 dataset. This last consists of 1400 binary images partitioned into 70 categories. Each category has 20 different shapes. For each class, 10 images are chosen as the test set and the remaining 10 images are then used for training. Despite the big number of classes, we chose the computation of overall classification to evaluate with accuracy the performance of our descriptor. We compared afterwards our results with those of SIFT descriptor . Table 3 shows that the overall classification accuracy of our descriptor on MPEG-7 dataset outperforms the one of SIFT. Overall classification was 86%. In order to analyze the classification results, we generated a confusion matrix which represents a matching matrix between the predicted class and the actual class (Fig. 8). We can see from confusion matrix that several objects were classified without any mistake. However, we can see from blue rectangles in the diagonal the few classes which are bad classified. These classes are: 15(chicken), 32 (device 9), 50 (jar).

Table 3: Overall accuracy on MPEG-7 dataset with training 50% and test 50%.

Training	Test	Overall Acuracy		
		SIFT(Setitra and Larabi, 2015)	RT	CRT
50%	50%	78%	75%	86%

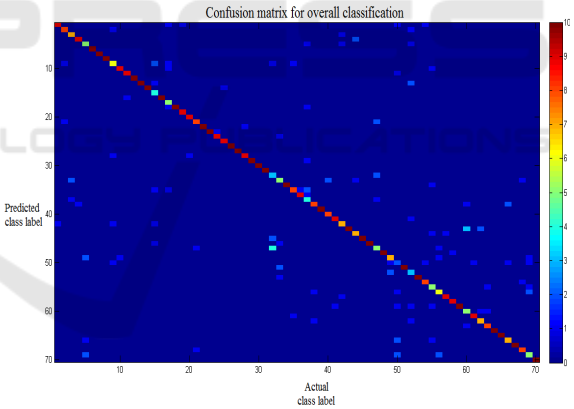

Figure 8: Confusion matrix for overall classification (MPEG-7 data set).

6 CONCLUSION

In this work we present a framework of the CRT which generalizes the classical RT by integrating a image function over conic sections. This makes it possible a new image analysis approach taking into account the global features of different (circular, parabolic, linear) shapes of analysed images. The interest and efficiency of the proposed approach is illustrated by numerical tests in feature extraction and object classification. The encouraging results open the

way to further research development directions taking into account more shapes of curves (ellipses, hyperbolas, etc.) and incomplete shapes (circular arcs, broken lines, etc.) of images under study (Nguyen and Truong, 2010) (Truong and Nguyen, 2015).

REFERENCES

Radon, J. (1917). Über die Bestimmung von Funktionen durch ihre Integralwerte längs gewisser Mannigfaltigkeiten. *Akad. Wiss.*, 69:262–277.

Ballard, D. (1981). Generalizing the hough transform to detect arbitrary shapes. *Pattern Recognition*, 13(2):111 – 122.

Bharath, B. V., Vilas, A. S., Manikantan, K., and Ramachandran, S. (2014). Iris recognition using Radon transform thresholding based feature extraction with Gradient-based Isolation as a pre-processing technique. In *2014 9th International Conference on Industrial and Information Systems (ICIIS)*, pages 1–8.

Chang, C.-C. and Lin, C.-J. (2011). LIBSVM: A library for support vector machines. *ACM Transactions on Intelligent Systems and Technology*, 2:27:1–27:27.

Cormack, A. M. (1981). The Radon transform on a family of curves in the plane. *Proceedings of the American Mathematical Society*, 83(2):325–330.

Elouedi, I., Fournier, R., Nat-Ali, A., and Hamouda, A. (2015). The polynomial discrete Radon transform. *Signal, Image and Video Processing*, 9(Supplement-1):145–154.

Hasegawa, M. and Tabbone, S. (2016). Histogram of Radon transform with angle correlation matrix for distortion invariant shape descriptor. *Neurocomputing*, 173:24–35.

Islam, S. and Sluzek, A. (2010). An evaluation of local image features for object class recognition. In *Proceedings of the International Conference on Computer Vision Theory and Applications (VISIGRAPP 2010)*, pages 519–523.

Lei, Y., Zheng, L., and Huang, J. (2014). Geometric invariant features in the Radon transform domain for near-duplicate image detection. *Pattern Recognition*, 47(11):3630–3640.

Nguyen, M. K. and Truong, T. T. (2010). Inversion of a new circular-arc Radon transform for Compton tomography. *Inverse Problems*, 26:065005.

Nguyen, T. P. and Hoang, T. V. (2015). Projection-Based Polygonality Measurement. *Image Processing, IEEE Transactions on*, 24(1):305–315.

Setitra, I. and Larabi, S. (2015). SIFT descriptor for binary shape discrimination, classification and matching. In *Computer Analysis of Images and Patterns - 16th International Conference, CAIP 2015, Valletta, Malta, September 2-4, 2015 Proceedings, Part I*, pages 489–500.

Truong, T. T. and Nguyen, M. K. (2015). New properties of the v-line Radon transform and their imaging applications. *Journal of Physics A: Mathematical and Theoretical*, 48(40):405204.

Zhang, D. and Lu, G. (2002). Shape-based image retrieval using generic Fourier descriptor. *Sig. Proc.: Image Comm.*, 17(10):825–848.

Zhang, Q. and Couloigner, I. (2007). Accurate Centerline Detection and Line Width Estimation of Thick Lines Using the Radon Transform. *IEEE Transactions on Image Processing*, 16(2):310–316.